Supporting Information

Mao et al. 10.1073/pnas.1719177115

SI Materials and Methods

Primary Cultures of Differentiated Human Airway Epithelia. Trachea and bronchi of nonsmoker lungs were obtained from the Iowa Donor Network. Airway epithelial cells were prepared by enzyme digestion and seeded onto collagen-coated semipermeable membranes (0.33-cm^2 Transwell inserts) and grown at the air–liquid interface, as previously described (1). Primary cultures of airway epithelia were used after they had differentiated and at least 14 d after seeding. Studies were approved by the University of Iowa Institutional Review Board. We also studied NIH 3T3 cells as a control for GLI1 immunostaining.

Immunocytochemistry. Primary cultures of differentiated airway epithelia were fixed in 4% paraformaldehyde (Electron Microscopy Sciences) for 15 min, followed by permeabilization with 0.1% Triton X-100 (Thermo Scientific) for 20 min. Following three washes with PBS, cells were treated with Superblock (Thermo Scientific) for 1 h at room temperature and then incubated with primary antibody overnight at 4 °C. After five washes with PBS, cells were treated with secondary antibodies for 45 min at room temperature. After PBS washing, filters were cut from their supports and mounted in Vectashield containing DAPI to label nuclei. Confocal *z*-series were acquired on an Olympus FluoView1000 or a Leica SP8 confocal microscope. Images were analyzed with NIH Fiji software. Primary antibodies are listed in Table S1. Secondary antibodies were Alexa Fluor goat anti-rabbit or anti-mouse and donkey anti-goat or anti-rabbit (Life Technologies; 1:500).

In assessing the antibodies we used, there were several considerations. First, many of the antibodies had been used previously to detect the human proteins in previous studies (Table S1). Second, for many of the HH signaling proteins, we used more than one antibody and obtained similar results (Table S1). Third, we verified the SMO localization with overexpressed SMO (Fig. S3*F*). Fourth, applications of secondary antibodies without primary antibody were negative for immunostaining. Fifth, antibodies from the same species showed different localization patterns when targeted to different proteins (Table S1). For example, rabbit polyclonal antibody to acetylated α-tubulin gave a different immunostaining pattern than rabbit polyclonal antibody to SMO, and rabbit polyclonal antibody to GLI1 showed no staining. Another example is that mouse monoclonal antibodies to SMO and adenylyl cyclase 5/6 both identified immunostaining in motile cilia, but punctate immunostaining was in adjacent rather than overlapping areas.

Immunostaining was performed and analyzed by S.M., A.S.S., and T.O.M. All studies were performed at least four times using epithelia prepared from different donors.

Transmission Electron Microscopy. Primary cultures of differentiated airway epithelia were rinsed with PBS and fixed with 2.5% gluteraldehyde in 0.1 M sodium cacodylate. Airway epithelia were then postfixed in 2% osmium tetroxide, en bloc-stained with 2.5% uranyl acetate, dehydrated through a graded ethanol series, infiltrated with Eponate 12 (Ted Pella), and polymerized at 60 °C for 24 h. Thin sections (70 nm) were cut on a Leica EM UC6 μLtramicrotome and counterstained with 5% uranyl acetate and Reynold's lead citrate before examination on a Jeol JEM-1230 transmission electron microscope. Images were captured using a Gatan 2k × 2k CCD camera.

Quantitative RT-PCR. Total RNA was isolated from primary cultures of differentiated human airway epithelia (RNeasy Lipid Tissue Mini kit; Qiagen). First-strand cDNA was synthesized with random primers (High Capacity cDNA Reverse Transcription Kit). Sequence-specific TaqMan probes for human *SHH*, *PTC1*, *SMO*, *GLI1-3*, *SUFU*, *PTC2*, and *β-actin* were from ABI (Table S2). Quantitative RT-PCR was performed with or without reverse-transcription enzyme in an ABI 7500 Fast Real-time PCR System. The PCR solution mix (10 μL) was run on a 1.5% agarose gel and imaged with UV light. To study the effect of stimuli on *GLI1* and *PTC1*, primary cultures of differentiated human airway epithelia were treated for 24 h with vehicle, 53-nM human recombinant SHH ligand (R&D Systems), or 100 nM SMO agonist SAG (EMD Millipore).

SHH Assay. To assay apical SHH, we washed the apical surface and changed to fresh basolateral medium. Seven days later, we collected the basolateral medium and apical surface liquid. To collect apical surface liquid, for epithelia from each donor, we applied 100 μL PBS to the apical surface of an airway epithelium, removed the liquid and transferred it to a second epithelium, and progressed through a total of six epithelia. At the end of the procedure, we had collected ∼60 μL of liquid. To assay SHH, we used a reporter cell line, Shh-LIGHT2 cells (2). Cells were cultured to confluence in 96-well plates and treated with the collected ASL, the basolateral medium, or various concentrations of SHH or other compounds in DMEM containing 0.5% (vol/vol) FBS. After 24 h incubation at 37 °C, cellular Firefly and *Renilla* luciferase activities were measured as described previously (2–4). For a standard curve, we constructed the relationship between the SHH concentration and the ratio of Firefly to *Renilla* luciferase activity. We used that curve to estimate the concentrations of SHH in the apical surface liquid and basolateral medium. We then calculated the rate of SHH secretion to the apical and basolateral surface.

GLI Assay. GLI transcriptional activity was measured with a firefly luciferase-based GLI-reporter assay. Primary cultures of differentiated human airway epithelia were studied 72 h after basolateral exposure to adenovirus encoding GliRELuciferase (Viral Vector Core Facility, University of Iowa). After 24-h interventions, cellular Firefly and *Renilla* luciferase activities were measured as described previously (2–5).

ELISA-Based cAMP Assay. The cAMP concentration of primary cultures of differentiated human airway epithelia was measured by ELISA according to the manufacturer's directions (Enzo Life). cAMP measurements were normalized to whole-cell protein concentrations quantitated by Protein BCA assay (Thermo Fisher).

FRET-Based cAMP Assay. Primary cultures of differentiated human airway epithelia were studied 72 h after basolateral exposure to adenovirus encoding SSTR3-Cerulean-mlCNBD-citrine (6). Epithelia were studied at 37 °C, and confocal images were collected on a Zeiss LSM 880 NLO using 440-nm excitation, with emissions bands centered on 482 nm (cerulean) and 544 nm (citrine). For each experiment, *z*-stacks consisting of three optical sections at 5-μm intervals were collected at 5-s intervals. Two to three ciliated cells expressing the transgene were imaged for each condition. Relative cAMP levels were calculated as the ratio of cerulean to citrine emissions at defined regions of interest using Zeiss Zen software.

CBF Measurement. CBFs were measured by transmitted light linescans on a Zeiss LSM 880 NLO using 488-nm illumination.

Primary cultures of differentiated human airway epithelia were placed on glass-bottom 35-mm dishes, and maintained at 37 °C. For each condition, two to three ciliated cells were randomly selected and scanned at ∼1,600 lines per second for a total of 2,000 lines. CBFs were calculated using NIH ImageJ software.

ASL pH Measurement. To measure ASL pH in primary cultures of airway epithelia, we used a fluorescent ratiometric pH indicator SNARF-1 conjugated to dextran (D-3304; Molecular Probes). SNARF suspended in perfluorocarbon was distributed onto the apical surface and ASL pH was assessed 2 h later (7, 8). Cultured airway epithelia were studied in a humidified, 5% CO_2 chamber at 37 °C on the stage of an inverted laser scanning microscope (Zeiss LSM 880 NLO). SNARF was excited at 514 nm, and fluorescence intensity was recorded at 561–606 nm and 623–695 nm. pH was calculated as previously described (7, 8).

Measurement of Transepithelial HCO_3^- Secretion. Primary differentiated cultures of airway epithelia were mounted in Ussing chambers (Physiologic Instruments). To study HCO_3^- transport, epithelia were bathed on both surfaces with Cl^--free solution containing: 118.9 mM NaGluconate, 25 mM $NaHCO_3$, 2.4 mM K_2HPO_4, 0.6 mM KH_2PO_4, 5 mM CaGluconate, 1 mM MgGluconate, and 5 mM dextrose, and gassed with 5% CO_2 (9). Short-circuit current (Isc) was measured under basal conditions and after the following apical additions: 100 μM amiloride, intervention (vehicle, SHH, SAG, cyclopamine-KAAD), forskolin, and IBMX, and 100 μM GlyH-101.

Reagents. In some experiments, the airway epithelia were incubated with various reagents, including the following. Human recombinant SHH ligand (R&D Systems) was applied to the apical surface at 53 nM for 24 h; this is in the range previously reported (10, 11) and consistent with our assay of ASL SHH concentration (Fig. S1*B*). SMO agonist SAG (EMD Millipore) was applied to the apical surface at 100 nM for 24 h for qRT-PCR and 200 nM for 20 min in other experiments; this is in the range previously reported (2, 3). Cyc-KAAD (EMD Millipore) was applied to the apical surface at 250 nM for 20 min; this is in the range previously reported (2, 11). Cyc-KAAD was added basolaterally for measurement of the effect on ASL pH. PTX (Sigma) was added to the basolateral medium at 1.7 nM overnight; this is in the range previously reported (11, 12). Forskolin (5 μM; Cayman Chemical) and IBMX (100 μM; Sigma) were also used.

An SSTR3-mlCNBD-FRET construct (6) was subcloned into TOPO-TA vector via EcoR I/Not I. The digested PCR products were further cloned into an adenoviral shuttle vector. Adenovirus encoding SSTR3-mlCNBD-FRET was generated by the University of Iowa Gene Transfer Vector Core. To overexpress SMO, we used an adenovirus 5 construct (3) from the University of Iowa Gene Transfer Vector Core. For gene transfer, we inverted the airway epithelial cultures and applied adenovirus (multiplicity of infection = 200) to the basolateral surface at 37 °C in 5% CO_2 for 30–45 min. Epithelia were assayed 72 h later.

Statistical Analysis. Statistical significance was tested with an unpaired or paired Student's t test for comparisons between two samples. For comparisons between more than two samples, statistical significance was tested with a one-way repeated-measures ANOVA with Sidak multiple-comparison posttest. $P < 0.05$ was considered statistically significant.

1. Karp PH, et al. (2002) *Epithelial Cell Culture Protocols*, ed Wise C (Humana Press, Totowa, NJ), pp 115–137.
2. Chen JK, Taipale J, Young KE, Maiti T, Beachy PA (2002) Small molecule modulation of Smoothened activity. *Proc Natl Acad Sci USA* 99:14071–14076.
3. Rohatgi R, Milenkovic L, Corcoran RB, Scott MP (2009) Hedgehog signal transduction by Smoothened: Pharmacologic evidence for a 2-step activation process. *Proc Natl Acad Sci USA* 106:3196–3201.
4. Hyman JM, et al. (2009) Small-molecule inhibitors reveal multiple strategies for hedgehog pathway blockade. *Proc Natl Acad Sci USA* 106:14132–14137.
5. Belgacem YH, Borodinsky LN (2015) Inversion of sonic hedgehog action on its canonical pathway by electrical activity. *Proc Natl Acad Sci USA* 112:4140–4145.
6. Mukherjee S, et al. (2016) A novel biosensor to study cAMP dynamics in cilia and flagella. *eLife* 5:e14052.
7. Pezzulo AA, et al. (2012) Reduced airway surface pH impairs bacterial killing in the porcine cystic fibrosis lung. *Nature* 487:109–113.
8. Tang XX, et al. (2016) Acidic pH increases airway surface liquid viscosity in cystic fibrosis. *J Clin Invest* 126:879–891.
9. Chen J-H, et al. (2010) Loss of anion transport without increased sodium absorption characterizes newborn porcine cystic fibrosis airway epithelia. *Cell* 143:911–923.
10. Shen F, Cheng L, Douglas AE, Riobo NA, Manning DR (2013) Smoothened is a fully competent activator of the heterotrimeric G protein G(i). *Mol Pharmacol* 83:691–697.
11. Polizio AH, et al. (2011) Heterotrimeric Gi proteins link Hedgehog signaling to activation of Rho small GTPases to promote fibroblast migration. *J Biol Chem* 286:19589–19596.
12. Moore BS, et al. (2016) Cilia have high cAMP levels that are inhibited by Sonic Hedgehog-regulated calcium dynamics. *Proc Natl Acad Sci USA* 113:13069–13074.

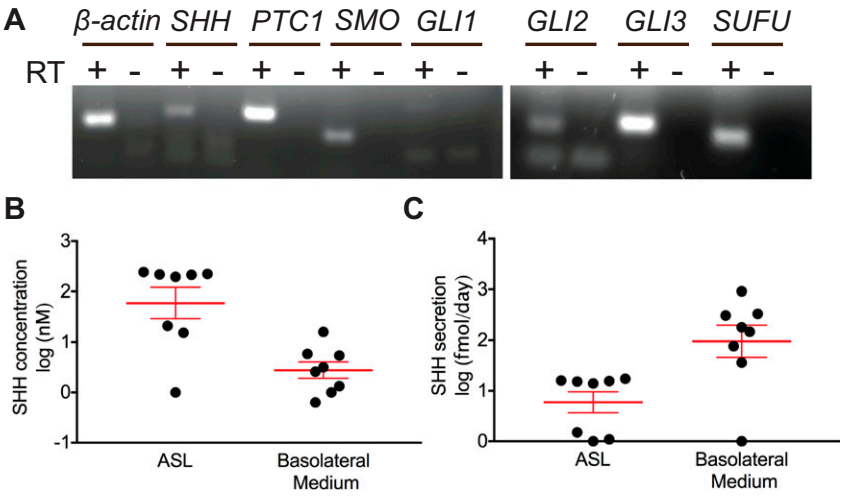

Fig. S1. SHH signaling pathway components are expressed in differentiated human airway epithelia and SHH is present in ASL. (*A*) RT-PCR analysis of mRNA expression of *β-actin*, *SHH*, *PTC1*, *SMO*, *GLI1*, *GLI2*, *GLI3*, and *SUFU* with and without reverse-transcriptase (RT). (*B*) SHH concentration in ASL and basolateral medium. (*C*) SHH secretion rate into ASL and basolateral medium. (*B* and *C*) The apical surface was washed and the basolateral medium was changed, and then SHH was allowed to accumulate for 7 d. After 7 d, we measured the SHH concentrations and calculated the secretion rates. Data are mean ± SEM, $n = 8$ donors. Although the rate of basolateral secretion exceeded the rate of apical secretion, the concentration of SHH was higher in the ASL because the volume of liquid is small. It is interesting that the rate of appearance of SHH in the basolateral medium is higher than in the apical medium even though we observe SHH predominantly in the apical portion of ciliated airway cells (Fig. 1*B*). Whether these rates are influenced by SHH movement from apical to basolateral compartments down the SHH concentration gradient, or direct secretion into the basolateral compartment remain unknown. The ASL SHH concentration is in the same range as that measured in nasal mucus samples (1) and in bronchoalveolar lavage liquid (2).

1. Henkin RI, Hosein S, Stateman WA, Knöppel AB, Abdelmeguid M (2017) Improved smell function with increased nasal mucus sonic hedgehog in hyposmic patients after treatment with oral theophylline. *Am J Otolaryngol* 38:143–147.
2. Cigna N, et al. (2012) The hedgehog system machinery controls transforming growth factor-β-dependent myofibroblastic differentiation in humans: Involvement in idiopathic pulmonary fibrosis. *Am J Pathol* 181:2126–2137.

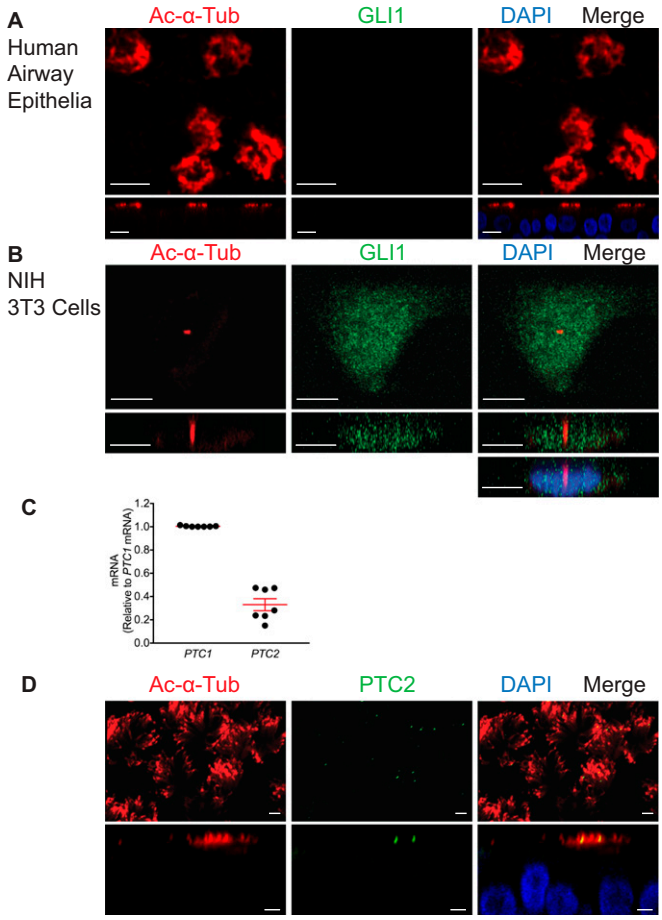

Fig. S2. GLI1 was not detected in ciliated airway epithelial cells and PTC2 was detected at lower levels than PTC1. (*A* and *B*) GLI1 is green, acetylated α-tubulin is red, and DAPI (nuclei) is blue. (Scale bars, 10 μm.) (*A*) Immunostaining did not detect GLI1 in ciliated airway epithelial cells. Data are *z*-series stacks of confocal images in the *X-Y* plane (*Upper*) and images in *X-Z* plane (*Lower*). (*B*) Immunostaining of GLI1 in an NIH 3T3 cell as a positive control. (Scale bars, 10 μm.) (*C*) qRT-PCR for *PTC1* and *PTC2* transcripts shown as value relative to *PTC1*. $n = 7$ different donors. (*D*) Immunostaining of acetylated α-tubulin is red, staining of PTC2 is green, and DAPI is blue. *Upper* images are shown in *X-Y* plane and *Lower* images are shown in *X-Z* plane. (Scale bars, 5 μm.)

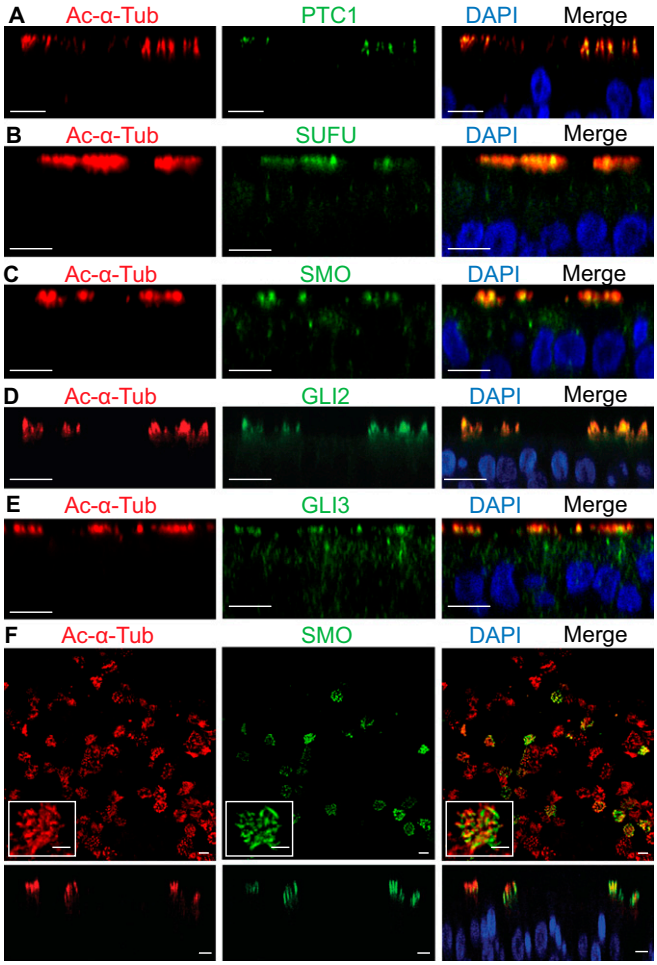

Fig. S3. HH signaling proteins are located in motile cilia on airway epithelia. (*A–E*) Staining of acetylated α-tubulin is red, staining of other immunolabeled proteins is green, and DAPI is blue. Immunostaining is for PTC1 (*A*), SUFU (*B*), SMO (*C*), GLI2 (*D*), and GLI3 (*E*). Images are shown in *X-Z* plane, (Scale bars, 10 μm.) (*F*) Overexpressed SMO localized in multiple motile cilia. Primary cultures of differentiated human airway epithelia were studied 72 h after basolateral exposure to adenovirus encoding SMO. Staining of acetylated α-tubulin is red, staining of SMO is green, and DAPI is blue. (*Upper*) A *z*-series stack of confocal images in the *X-Y* plane; (*Lower*) images in *X-Z* plane. (Scale bars, 10 μm.) (*Insets*) One cell (Scale bar, 5 μm.)

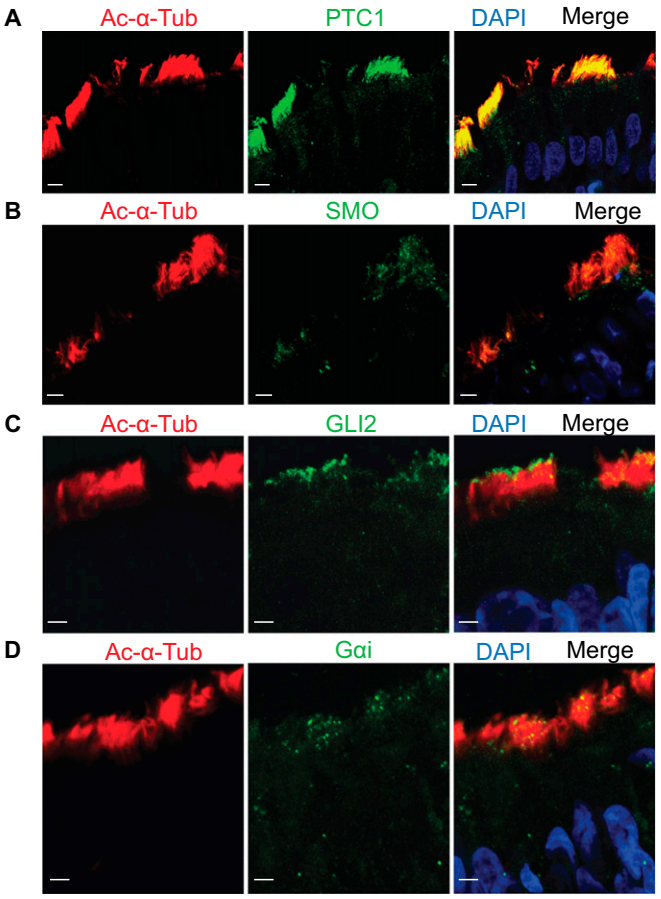

Fig. S4. HH and cAMP signaling components are located in airway motile cilia of lung tissue. (*A–D*) Staining of acetylated α-tubulin is red, staining of other immunolabeled proteins is green, and DAPI is blue. Immunostaining is for PTC1 (*A*), SMO (*B*), GLI2 (*C*), and $G\alpha_i$ (*D*). Data are confocal images in *X-Z* plane. (Scale bars, 5 μm.)

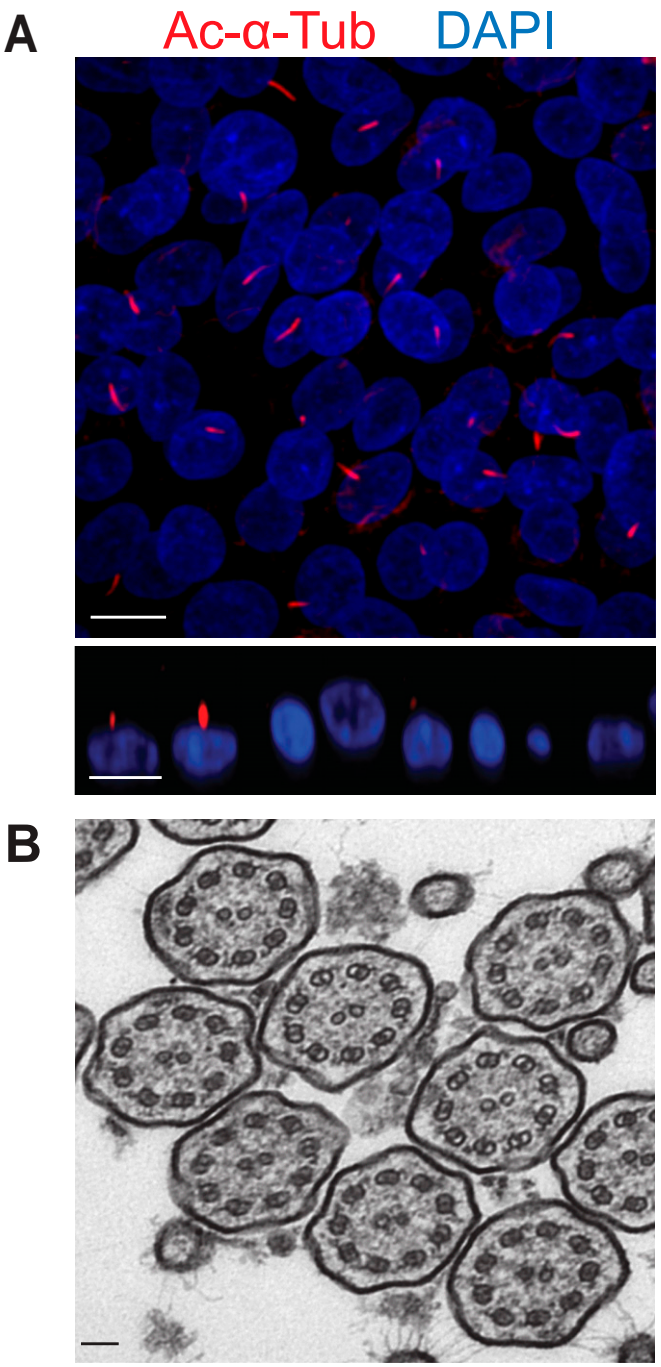

Fig. S5. Undifferentiated airway epithelial cells have primary cilia and differentiated human airway epithelial cells have a "9 + 2" axoneme. (*A*) Epithelial cells were immunostained 6 d after seeding and before the development of a differentiated epithelium. Acetylated α-tubulin (red) and DAPI (blue). (Scale bars, 10 μm.) (*Upper*) Stack of *X-Y* confocal immunofluorescence images; (*Lower*) *X-Z* image. Similar results have been reported previously (1). (*B*) Transmission electron micrograph of cross-section of cilia on airway epithelial cell. (Scale bar, 100 nm.)

1. Jain R, et al. (2010) Temporal relationship between primary and motile ciliogenesis in airway epithelial cells. *Am J Respir Cell Mol Biol* 43:731–739.

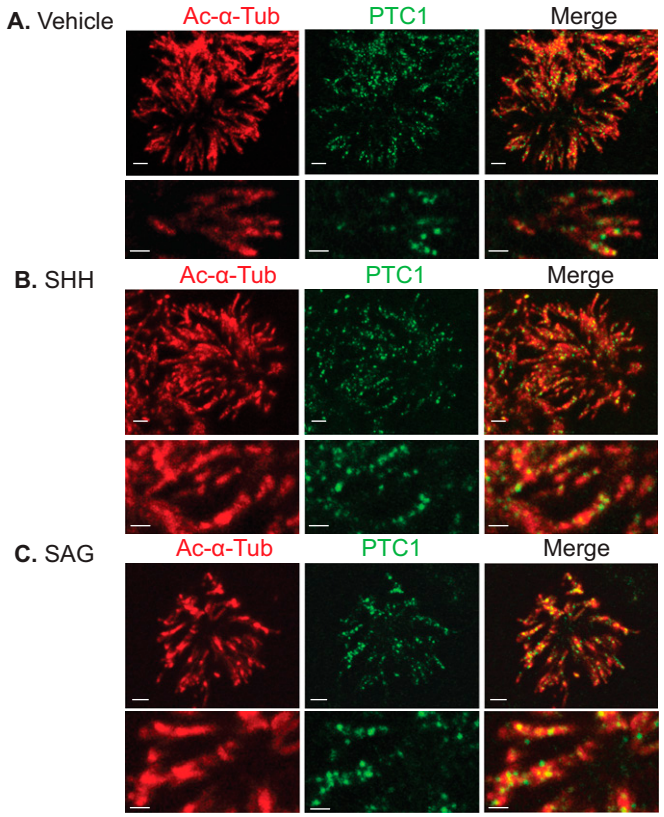

Fig. S6. SHH and SAG did not alter the cellular location of PTC1. Data are immunocytochemical images of differentiated human airway epithelia. Localization of PTC1 (green) and acetylated α-tubulin (red). Epithelia were treated with (*A*) vehicle, (*B*) SHH (53 nM), and (*C*) SAG (100 nM), all for 24 h. *Lower* images are expanded images from *Upper* images. [Scale bars: 2 μm (*Upper*); 1 μm (*Lower*).]

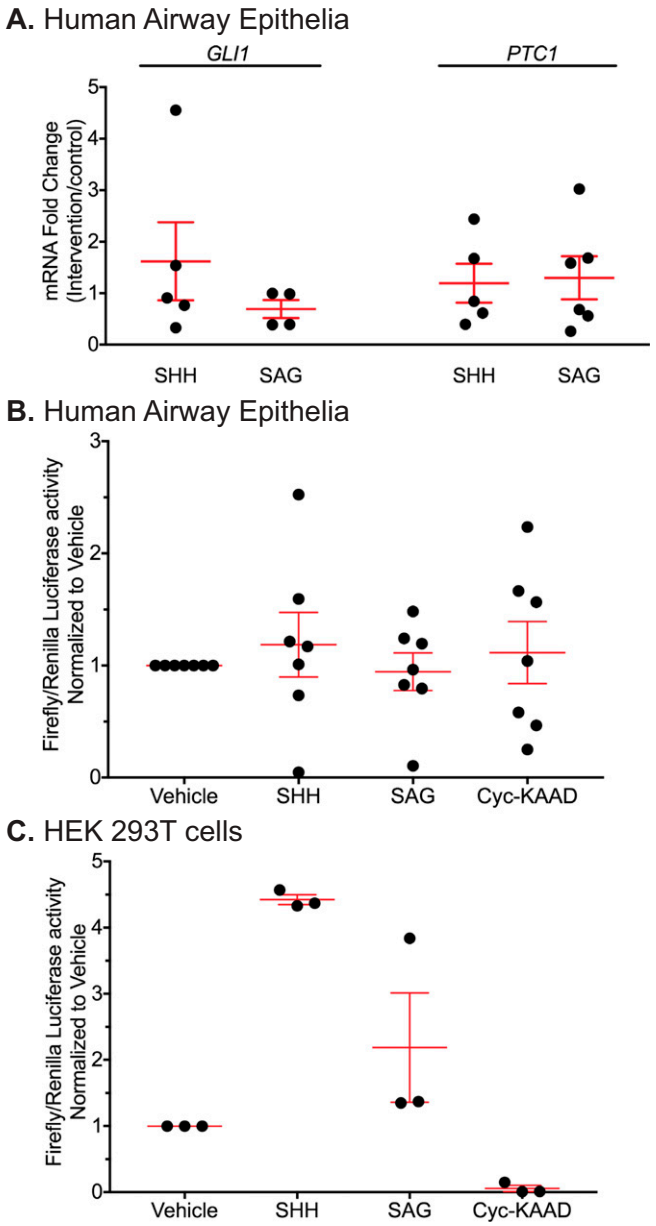

Fig. S7. SHH and SAG did not alter PTC1 or GLI1 transcript levels. (*A*) Data are qRT-PCR levels of PTC1 and GLI1 mRNA. Data are fold-change for epithelia treated with the intervention relative to epithelia treated with paired vehicle controls. Interventions were SHH (53 nM) and SAG (100 nM) applied for 24 h. Each data point is mean of two to three epithelial cultures from a different donor. Bars and whiskers are mean ± SEM. $n = 4$–6 donors for each condition. (*B*) Data are assay of GLI transcriptional activity measured with a GLI-luciferase reporter. Data are fold-change of firefly luciferase (driven by the GLI1 promoter) normalized to *Renilla* luciferase (driven by a CMV promoter) for human airway epithelia treated with the intervention relative to epithelia treated with vehicle controls. Interventions were SHH (53 nM), SAG (100 nM), and Cyc-KAAD (250 nM) applied for 24 h. Each data point is mean of two epithelial cultures from a different donor. Bars and whiskers are mean ± SEM. $n = 7$ donors for each condition. (*C*) As a positive control, in HEK 293T cells, SHH (53 nM) and SAG (100 nM) increased and Cyc-KAAD (250 nM) decreased the ratio of firefly to *Renilla* luciferase activity. $n = 3$ for each condition.

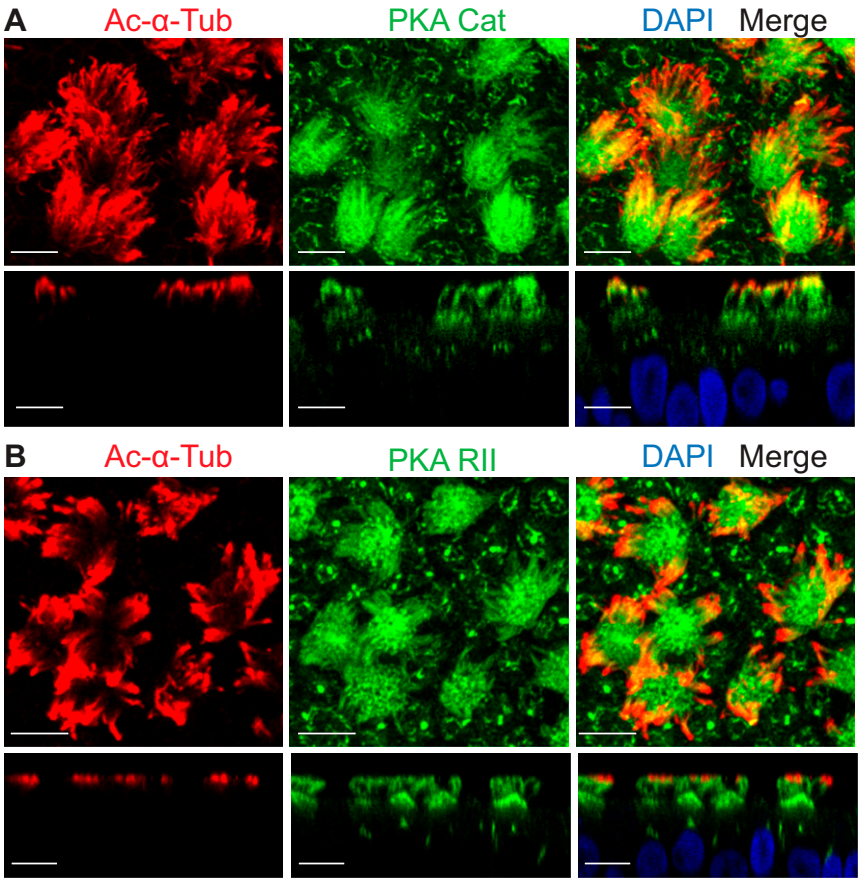

Fig. S8. cAMP-dependent PKA subunits are located in motile cilia of human airway epithelial. Staining of acetylated α-tubulin is red, staining of PKA subunits are green, and DAPI is blue. (*A*) Catalytic subunit of PKA. (*B*) Regulatory II subunit of PKA. (*Upper*) A *z*-series stack of confocal images in the *X-Y* plane; (*Lower*) images in the *X-Z* plane. (Scale bars, 10 μm.)

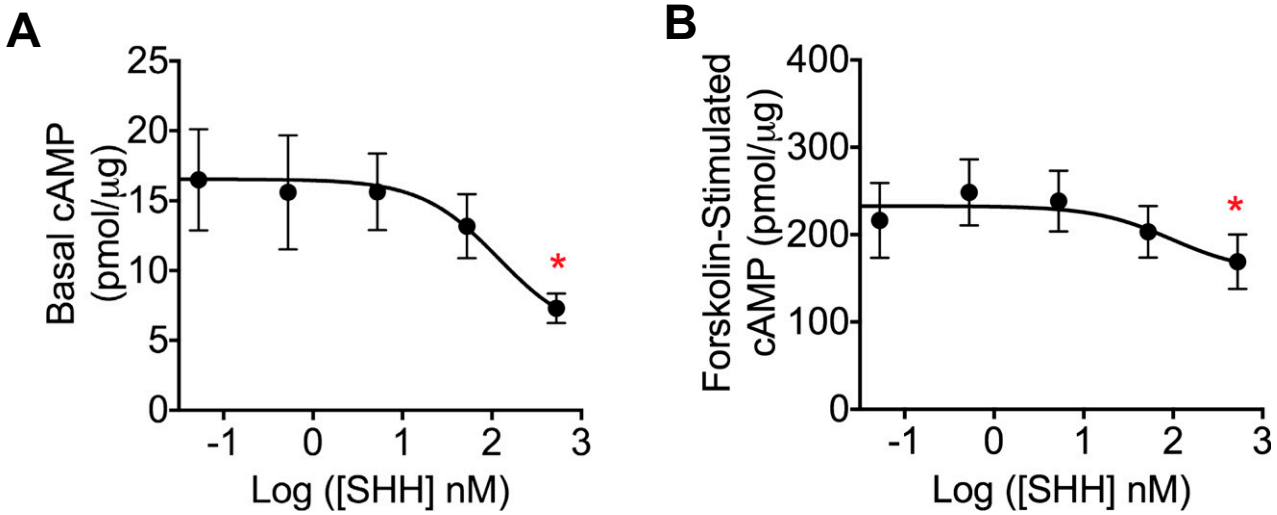

Fig. S9. SHH decreased basal and forskolin-stimulated intracellular levels of cAMP. Data are cAMP concentrations in differentiated human airway epithelia under (*A*) basal conditions, and (*B*) 10 min after addition of forskolin (5 μM) and IBMX (100 μM). Epithelia received increasing concentrations of SHH. Data are mean ± SEM. $n = 6$ donors. An asterisk (*) indicates difference from control (no SHH), $P < 0.05$ by one-way repeated-measures ANOVA with Sidak multiple-comparison posttest. Under basal conditions and after applying forskolin to stimulate adenylyl cyclase, the EC_{50} was 2.6 μg/mL and 2.9 μg/mL, respectively. These values are in the same range as reported for primary cilia (1).

1. Shen F, Cheng L, Douglas AE, Riobo NA, Manning DR (2013) Smoothened is a fully competent activator of the heterotrimeric G protein G(i). *Mol Pharmacol* 83:691–697.

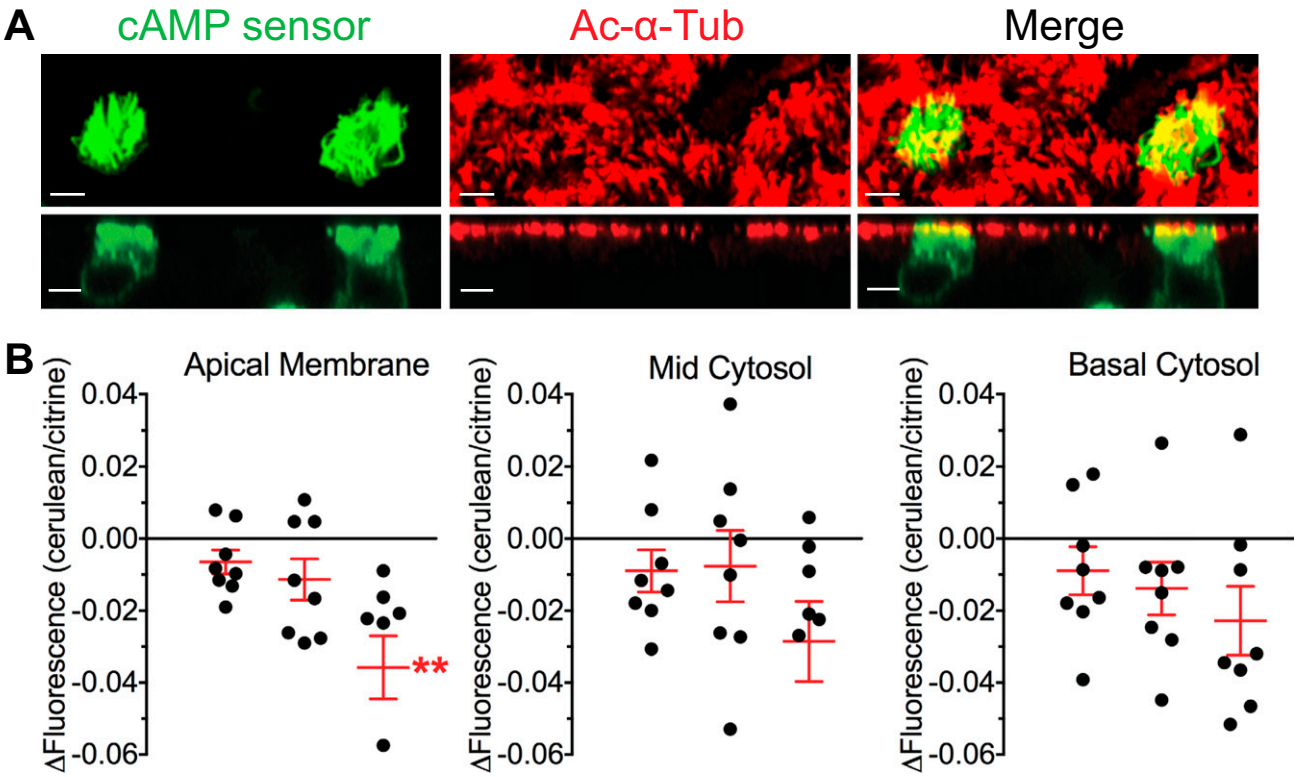

Fig. S10. SHH did not decrease intracellular levels of cAMP in nonciliated cells. (*A*) Immunostaining of a cAMP sensor (green) expressed in a ciliated cell (acetylated α-tubulin, red). (*Upper*) Stack of *X-Y* images; (*Lower*) *X-Z* images. (Scale bar, 5 μm.) (*B*) Change in cerulean/citrine fluorescence ratio of the FRET-based cAMP sensor in nonciliated cells at the level of apical membrane, in the midportion of the cell, and at the basal region of the cell. These data are from the same experiment as in Fig. 4*C*, but were in nonciliated cells in the same microscopic field. Fluorescence is reported 15 min after addition of vehicle, SHH (263 nM), or MDL-12330A (100 μM, as a positive control). Each data point is the average of two to three nonciliated cells in epithelia from a different donor. $^{**}P < 0.01$ compared with vehicle by one-way repeated-measures ANOVA with Sidak multiple-comparison posttest.

Table S1. Primary and secondary antibodies used for immunostaining

Protein	Vendor	Product no.	Type	Dilution	Figure	Refs. in human study
SHH	Santa Cruz	1194	Goat polyclonal against N terminus	1:100	Fig. 1*B*	(1, 2)
PTC1	Abcam	39266	Rabbit monoclonal against residue 500–600	1:100	Fig. 2*A* and Fig. S3*A*	(3)
PTC1	Thermo Scientific	PA1-46222,	Rabbit polyclonal	1:100	Fig. 3*A*, and Figs. S4*A* and S6 *A*–*C*	
SUFU	Abcam		Rabbit monoclonal	1:100	–	
SUFU	Santa Cruz	137014	Mouse monoclonal	1:100	Fig. 2*B* and Fig. S3*B*	(4)
SMO	LSBio	A2668	Rabbit polyclonal against N terminus	1:100	Figs. 2*C* and 3*D*, and Figs. S3 *C* and *F*, and S4*B*	(5)
SMO	LSBio	A2666	Rabbit polyclonal against N terminus	1:100	–	(6)
SMO	Abcam	38686	Rabbit polyclonal against C terminus	1:100	–	(5)
SMO	LifeSpan	B6399	Mouse monoclonal	1:50	Fig. 3 *A* and *E*	
GLI1	Santa Cruz	20687	Rabbit polyclonal	1:100	Fig. S2 *A* and *B*	(7, 8)
GLI1	Santa Cruz	515751	Mouse monoclonal	1:100	–	
GLI2	Santa Cruz	20290	Goat polyclonal against N terminus	1:100	Fig. 2*D* and Figs. S3*D* and S4*C*	(5, 9)
GLI2	Santa Cruz	28674	Rabbit polyclonal against C terminus	1:100	–	(5, 9)
GLI3	Santa Cruz	6155	Goat polyclonal against N terminus	1:100	Fig. 2*E* and Fig. S3*E*	(5, 10)
GLI3	Santa Cruz	74478	Mouse monoclonal against N terminus	1:100	–	
Adenylyl cyclase 5/6	Santa Cruz	590	Rabbit polyclonal against C terminus	1:100	Fig. 3 *C* and *E*	(11)
Adenylyl cyclase 5/6	Santa Cruz	514785	Mouse monoclonal against C terminus	1:100	–	
$G\alpha_{i\text{-}1/2/3}$	Santa Cruz	26761	Goat polyclonal against N terminus	1:100	Fig. 3 *B* and *D* and Fig. S4*D*	(12)
$G\alpha_{i\text{-}1/2/3}$	Santa Cruz	136478	Mouse monoclonal against N terminus	1:100	–	
PKAα catalytic subunit	Santa Cruz	903	Rabbit polyclonal against C terminus	1:100	Fig. S8*A*	(13)
PKA IIα regulatory subunit	Santa Cruz	908	Rabbit polyclonal against C terminus	1:100	Fig. S8*B*	(14)
Acetylated α-Tubulin	Cell Signaling	5335	Rabbit monoclonal	1:300	*	(15)
Acetylated α-Tubulin	Life Technology	322700	Mouse monoclonal	1:200	*	(16)
IFT88	Thermo Scientific	PA5-18467	Goat polyclonal	1:100	Fig. 3*A*	(17)
PTC2	R&D system	403438	Mouse monoclonal	1:100	Fig. S2*D*	
Alexa Fluor goat anti-rabbit or anti-mouse	Life Technologies			1:500	†	
Alexa Fluor donkey anti-goat, anti-rabbit, or anti-mouse	Life Technologies			1:500	†	

Antibodies are listed by protein, vendor, product number, type, and dilution. "–" indicates that data using that antibody are not in the figures.
*Indicates that the antibody to acetylated α-tubulin that we used depended on the species of the other primary antibody.
†Indicates that the secondary antibody that we used depended on the species of the primary antibody. Note that because *adenylyl cyclase 6* mRNA is more abundant than *adenylyl cyclase 5* mRNA in airway epithelia (18, 19), the antibody may be detecting adenylyl cyclase 6.

1. van den Brink GR, et al. (2001) Sonic hedgehog regulates gastric gland morphogenesis in man and mouse. *Gastroenterology* 121:317–328.
2. Jenkins D, Winyard PJ, Woolf AS (2007) Immunohistochemical analysis of sonic hedgehog signalling in normal human urinary tract development. *J Anat* 211:620–629.
3. Sun Y, et al. (2014) Gli1 inhibition suppressed cell growth and cell cycle progression and induced apoptosis as well as autophagy depending on ERK1/2 activity in human chondrosarcoma cells. *Cell Death Dis*, 10.1038/cddis.2013.497.
4. Drannik A, et al. (2017) Cerebrospinal fluid from patients with amyotrophic lateral sclerosis inhibits sonic hedgehog function. *PLoS One* 12:e0171668.
5. Nielsen SK, et al. (2008) Characterization of primary cilia and hedgehog signaling during development of the human pancreas and in human pancreatic duct cancer cell lines. *Dev Dyn* 237:2039–2052.
6. Zhu G, et al. (2007) Sonic and desert hedgehog signaling in human fetal prostate development. *Prostate* 67:674–684.
7. Cui W, et al. (2010) Expression and regulation mechanisms of sonic hedgehog in breast cancer. *Cancer Sci* 101:927–933.
8. Savani M, Guo Y, Carbone DP, Csiki I (2012) Sonic hedgehog pathway expression in non-small cell lung cancer. *Ther Adv Med Oncol* 4:225–233.
9. Bishop CL, et al. (2010) Primary cilium-dependent and -independent hedgehog signaling inhibits p16(INK4A). *Mol Cell* 40:533–547.
10. Alinger B, et al. (2009) Hedgehog signaling is involved in differentiation of normal colonic tissue rather than in tumor proliferation. *Virchows Arch* 454:369–379.
11. Vuolo L, Herrera A, Torroba B, Menendez A, Pons S (2015) Ciliary adenylyl cyclases control the hedgehog pathway. *J Cell Sci* 128:2928–2937.
12. García-Bernal D, et al. (2011) RGS10 restricts upregulation by chemokines of T cell adhesion mediated by $\alpha 4\beta 1$ and $\alpha L\beta 2$ integrins. *J Immunol* 187:1264–1272.

13. Ma MPC, Thomson M (2012) Protein kinase A subunit α catalytic and A kinase anchoring protein 79 in human placental mitochondria. *Open Biochem J* 6:23–30.
14. Nguyen E, et al. (2013) Activation of both protein kinase A (PKA) type I and PKA type II isozymes is required for retinoid-induced maturation of acute promyelocytic leukemia cells. *Mol Pharmacol* 83:1057–1065.
15. Yan Y, et al. (2016) Human nasal epithelial cells derived from multiple subjects exhibit differential responses to H3N2 influenza virus infection in vitro. *J Allergy Clin Immunol* 138:276–281.e15.
16. Grati M, et al. (2015) A missense mutation in DCDC2 causes human recessive deafness DFNB66, likely by interfering with sensory hair cell and supporting cell cilia length regulation. *Hum Mol Genet* 24:2482–2491.
17. Kim H, et al. (2014) Ciliary membrane proteins traffic through the Golgi via a Rabep1/GGA1/Arl3-dependent mechanism. *Nat Commun* 5:5482.
18. Carolan BJ, et al. (2006) Up-regulation of expression of the ubiquitin carboxyl-terminal hydrolase L1 gene in human airway epithelium of cigarette smokers. *Cancer Res* 66:10729–10740.
19. Pezzulo AA, et al. (2011) The air-liquid interface and use of primary cell cultures are important to recapitulate the transcriptional profile of in vivo airway epithelia. *Am J Physiol Lung Cell Mol Physiol* 300:L25–L31.

Table S2. Primers used for quantitative RT-PCR

Gene	Product no.	Exon boundary
β-actin	Hs01060665_g1	2–3
SHH	Hs00179843_m1	2–3
PTC1	Hs00181117_m1	19–20
SMO	Hs01090242_m1	8–9
SUFU	Hs00960520_m1	3–4
GLI1	Hs01110776_g1	7–8
GLI2	Hs01119974_m1	6–7
GLI3	Hs00609233_m1	6–7
PTC2	Hs00184804_m1	19–20

Primers are listed by gene, product number (ABI), and exon boundary.

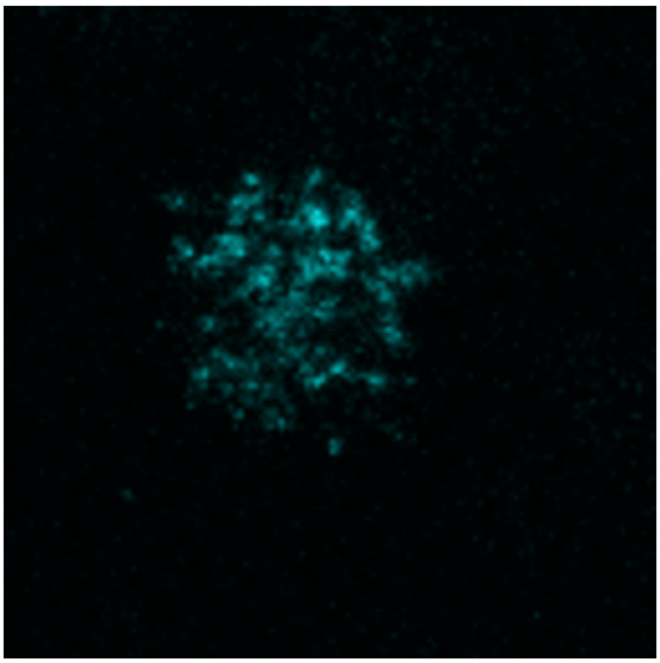

Movie S1. Movie of ciliated cell in a primary culture of human airway epithelia. The ciliated cell is expressing the cAMP sensor. The image is a single *X-Y* confocal plane at the level of the cilia. Video images were acquired at 482 nm (cerulean) and at 37 Hz. The 4-s video is shown in real time. This is the plane at which the FRET-based cAMP sensor was recorded for assessing changes in cAMP at the level of cilia in Fig. S10*A*. The dimensions of the image are 32 μm × 32 μm.

Movie S1